Two new Zn(II)/Cu(II) compounds: photoluminescent and photocatalytic properties, and protective activity on Parkinson disease

Ning Wang
Tsinghua University
Fang-Jie Huang
Tsinghua University
Mang-Suo Zhao
Tsinghua University
Bing-Xin Shi
Tsinghua University
Yan Wei
Tsinghua University
Li-Yan Qiao (okj301869@163.com)
Tsinghua University https://orcid.org/0000-0002-3640-7430

Research Article

Keywords: Cu(II) compound, Supramolecular framework, Luminescence, Photocatalysis, Parkinson's disease

Posted Date: July 7th, 2021

DOI: https://doi.org/10.21203/rs.3.rs-585571/v1

Abstract

Two coordination polymers, that is $[Zn(pdc)(im)(H_2O)]_n$ (**1**) and $[Cu(pdc)(im)_2]_n \cdot n(H_2pdc)$ (**2**) (H_2pdc = terephthalic acid, im = imidazole), were hydrothermally synthesized *via* the reactions of H_2pdc and im in combination with Zn(II) or Cu(II) ions. Compound **1** shows intense blue luminescence and compound **2** shows good photocatalytic activity for the methyl violet degradation under the irradiation of ultraviolet light. In addition, the assessment of the two compounds' application values against Parkinson's disease (PD) were carried out and their specific mechanism was tested simultaneously. First of all, the real time RT-PCR was implemented and the relative expression levels of NMDA receptor on neurons were measured. Besides, the Annexin V-FITC/PI apoptosis assay was utilized for the assessment of the influence of the compounds on the dopaminergic neuron death rate.

Introduction

Parkinson's disease (PD) is a type of common neurodegenerative disease in the middle-aged people and elderly. And the clinical characteristics of this disease are muscle stiffness, static tremor, bradykinesia, postural instability together with the lack of movement [1]. For the PD, the principal pathological change is the dopaminergic neurons loss in midbrain substantia nigra. Aspartic acid is an endogenous excitatory amino acid, which reveals a significant effect in the central nervous system of mammals [2, 3]. There is evidence that Parkinson's disease is related to the excessive accumulation of excitatory amino acids in the brain.

Recently, coordination polymers with novel compositions and topological frameworks have attracted great attention mainly owing to their functional properties that make them can be served as potential hybrid materials in catalysis, luminescence, magnetism, gas separation and storage, and other areas [4–7]. For creating the coordination polymers, one of the most effective method is the technology of hydrothermal or solvothermal self-assembly that requires intelligent selection of organic ligand with appropriate central metal ions and coordination positions having the definite coordination structures [8–11]. During the past few decades, organic carboxylate ligands as one kind of organic building backbone have been widespread exploited for producing the metal-organic coordination polymers with charming topological networks and attractive performances owing to their a variety of coordination manners of the carboxyl groups along with strong coordination affinity to metal centers [12–16]. Terephthalic acid (H_2pdc), as an inexpensive ligand, is a rigid aromatic carboxylate ligand and has four potential coordination sites. In the construction of coordination polymers, it usually acts as linear connectors, which is helpful for us to obtain the compounds with expected structures [17–19]. To date, numerous of single-nuclear or polynuclear metal-based coordination polymers with H_2pdc or H_2pdc and N-donor auxiliar ligands as organic backbone have been reported, which show excellent properties in gas storage, catalysis, and luminescence, etc [20–22]. In order to continue to develop new hybrid functional materials, in this work, terephthalic acid was selected to self-assemble with Zn(II) or Cu(II) ions using imidazole as the organic base to tune the reaction pH, successfully obtaining two coordination polymers, that is

$[Cu(pdc)(im)_2]_n \cdot n(H_2pdc)$ (**2**) and $[Zn(pdc)(im)(H_2O)]_n$ (**1**) (H_2pdc = terephthalic acid, im = imidazole). In the following, the syntheses, crystal structures, thermal behaviors, luminescent and photocatalytic properties will be reported. Their treatment effect on the PD was explored and the relevant mechanism was also explored.

Experimental

Materials and instrumentation

All of the raw chemical reagents employed in our investigation were acquired from Jinan Henghua Company, and they could be utilized directly. Vario EL III analyzer was employed for the analysis of Hydrogen, Nitrogen and Carbon elements for 1–2. The diffractometer of PANalytical X'Pert Pro was applied for the analysis of PXRD with 0.05° step size using the Cu/Kαradiation (with λ of 1.54056 Å). The two compounds' TGA were finished through employing the NETSCHZ STA-449C under flow of nitrogen at $10℃ \cdot min^{-1}$ heating rate in the temperature range of 30–800℃. The photocatalyticexperiments were carried out in a Persee TU-1950 UV-vis spectrophotometer. The luminescent spectra was measured using the fluorescence spectrophotometer of Edinburg FLS920 TCSPC under ambient temperature.

Synthesis of $[Zn(pdc)(im)(H_2O)]_n$ (1) and $[Cu(pdc)(im)_2]_n \cdot n(H_2pdc)$ (2)

The mixture generated from 0.2 mmol $Zn(NO_3)_2 \cdot 6H_2O$, 0.2 mmol H_2pdc, 0.2 mmol imidazole, and 8 mL H_2O was sealed to the stainless steel vessel (25 mL) lining with Teflon and the acquiring product was heated for three days under 160 ℃ temperature. Subsequently, it was naturally cooled to environmental temperature, the **1**'s colorless massive crystals were gained with 46 percent yield on the basis of $Zn(NO_3)_2 \cdot 6H_2O$. Anal. calcd. (%) for the $C_{11}H_{10}N_2O_5Zn$: N, 8.87, C, 41.83 and H, 3.17. Found (%): N, 8.91, C, 41.79 and H, 3.15.

The mixture generated from 0.1 mmol $Cu(NO_3)_2 \cdot 3H_2O$, 0.1 mmol H_2pdc, 0.2 mmol 4-bpmh, and 8 mL H_2O was sealed to the stainless steel container (25 mL) lining with Teflon and the acquiring mixture was heated for three days under 160 ℃ temperature. Subsequently, it was gradually cooled to ambient temperature, the **2**'s blue massive crystals were acquired with 52 percent yield according to $Cu(NO_3)_2 \cdot 3H_2O$. Anal. calcd. (%) for the $C_{22}H_{18}N_4O_8Cu$: N, 10.57, C, 49.82 and H, 3.40. Found (%): N, 10.55, C, 49.79 and H, 3.42.

X-ray crystallography

The architectural data of single crystal for the two compounds were harvested through the graphite–monochromated Mo–*Kα* radiation (with *λ* of 0.71073 Å) via exploiting the Mercury CCD controlled via the computer at ambient temperature. By utilizing the dual direct means, the compounds' architectures can be solved with *ShelXS*, and then the *SHELXL*-2014 is applied for the refinement of the structures via full-

matrix least square technique on the basis of F^2 [23]. The data of crystallography and the optimization of structures for the complexes were concluded in the Table 1. The chose bond angles (º) and lengths (Å) of the compounds are exhibited in the Table S1. The detailed parameters of H-bond for the complexes are displayed in the Table S2.

Table 1
The data of crystallography and the optimization of structures for the complexes.

Sample	**1**	**2**
Formula	$C_{11}H_{10}N_2O_5Zn$	$C_{22}H_{18}N_4O_8Cu$
Fw	315.58	529.94
Crystal system	monoclinic	triclinic
Space group	$P2_1/n$	$P\bar{1}$
a (Å)	7.9810(7)	8.312(2)
b (Å)	9.1811(7)	8.424(2)
c (Å)	16.3930(12)	16.254(4)
α(°)	90	87.985(6)
β(°)	90.659(4)	83.514(5)
γ(°)	90	80.767(5)
Volume ($Å^3$)	1201.11(16)	1116.0(5)
Z	4	2
Density (calculated)	1.745	1.577
Abs. coeff. (mm^{-1})	2.063	1.036
Total reflections	8831	8733
Unique reflections	2702	5035
Goodness of fit on F^2	1.174	1.042
Final *R* indices [$I > 2\text{sigma}(I^2)$]	$R = 0.0489$, $wR_2 = 0.1170$	$R = 0.0297$, $wR_2 = 0.0764$
R (all data)	$R = 0.0509$, $wR_2 = 0.1178$	$R = 0.0370$, $wR_2 = 0.0814$
CCDC	2087327	2087328

Real time RT-PCR

In our present investigation, the real time RT-PCR was finished to determine the expression levels of NMDA receptor on the neurons after the treatment of compounds. This conduction was implemented completely in accordance with instructions with only minor modification. In short, forty mice (4–5 weeks, 20–22g) were offered via the Model Animal Reach Center of Wuhan University (Wuhan, China). All of the mice applied in this research were maintained between 20 and 25℃, under the environment of free food and water. After that the PD animal model was established by the injection of β-amyloid, and treatment was performed with the two compounds at 5 mg each kg concentration. After that the neurons were separated, and then the TRIZOL was applied for the extraction of the entire RNA in cells. After measuring the entire RNA concentration, this concentration could be reverse transcripted into the cDNA. Ultimately, the relative expression of NMDA receptor against neurons was checked with the real time RT-PCR, in which the *gapdh* was employed as an internal control. This study was implemented for 3 times.

Annexin V-FITC/PI apoptosis assay

After β-amyloid stimulation, the evaluation of novel compounds' inhibitory influence against the apoptosis levels of neurons was conducted with Annexin V-FITC/PI apoptosis assay. All the implementation in our experiment was carried out on the basis of instructions. In general, in the phase of exponential growth, the neurons could be harvested and subsequently they were seeded with 2×10^5 cells per well destiny into the plates of 6-well, and they were cultivated in 5 percent of CO_2 humidified surroundings overnight at 37 ℃. Subsequently, the cells were treated through the two compounds with 5 mg per mL concentration for one day. Dimethyl sulfoxide (0.1 percent, DMSO) together with the apoptosis inducer kit (Beyotime, Shanghai, China) were exploited as a negative and positive control, respectively. Each of the group has 3 parallel wells. After the above treatment, in each group, the cells was collected and after that they were labeled via the application of propidium iodide (PI, 5 μL) along with Annexin V-FITC (5 μL) for thirty minutes. The determination of stained cells in each group was carried out by glow cytometry (BD, NJ, USA) at 488 nm excitation wavelength and 625 nm emission and 525 nm emission wavelength. The study requires to be finished at least 3 times.

Results And Discussion

Crystal structure of compound 1

The architectural research of X-ray single crystal indicated that the **1**'s architecture reflects an one-dimensional infinite chain based on $\{ZnO_3N\}$ nodes and pdc^{2-} linkers. And its fundamental unit is constructed from a Zn(II) ion, a ligand of pdc^{2-}, a terminal ligand of im together with a coordinated molecule of water. As illustrated in the Fig. 1, each of Zn(II) ion exhibits a coordination structure of tetrahedron, which is defined via 2 carboxylic acid O atoms in 2 diverse ligands of pdc^{2-}, a N atom originated from a terminal ligand of im and a coordinated molecule of water, and the bond separation of Zn-O/N are between 1.962(3) and 1.992(3) Å, and it is in a normal range [24]. These tetrahedral Zn(II) ions are linked through the ligands of pdc^{2-} by the carboxylic acid groups with the uniform monodentate manner to provide an one-dimensional infinite zigzag chain architecture (Fig. 1b), and the Zn…Zn

separated by pdc^{2-} ligand is 11.01 Å. The H atoms of the suspended terminal im ligands in the chain can be suitably accepted via the carboxylic acid O atoms in the neighboring chains, producing the intermolecular H-bonds of N-H…O. These H-bonds of N□H…O linked the one-dimensional chains into a 2D layer motif with (4,4) grids (Fig. 1c). Interestingly, two adjacent hydrogen-bonded 2D layers interpenetrated with each other, forming an interpenetrated bi-layer structure (Fig. 2d). Also, the H donors of coordinated water molecules in these bi-layer structure can be appropriately accepted through the carboxylic acid O atoms derived from the consecutive bi-layer architecture. As a result, this bi-layers are in-depth H-bonded into a three-dimensional supramolecular skeleton (Fig. 1e). The corresponding hydrogen bond parameters can be found from the Table S2.

Crystal structure of compound 2

The diffraction of X-ray single crystal confirmed that the **2**'s fundamental unit is composed of 2 Cu(II) ions with the occupation ratio of 0.5, and a ligand of pdc^{2-}, two terminal im ligands, as well as one free H_2pdc molecule. As displayed in the Fig. 2a, the Cu1 ion and Cu2 ion are both tetracoordinated via 2 carboxylic acid O atoms in 2 diverse ligands of pdc^{2-} and 2 N atoms come from 2 terminal on a basal level, and the spacing of Cu-O/N are between 1.9436(14) and 1.9759(17), which is also in a normal range. On account of the well-known John-Teller effect of Cu(II) ion with d^9 electronic configuration, the coordination geometries of Cu(II) ions can be described as elongated octahedrons with the axial sites taken over via the 2 carboxylic acid O atoms in 2 distinct ligands of H_2pdc, and the weak distances of Cu…O are from 2.870 to 2.970 Å. The pdc^{2-} ligands in **2** act as μ_2-bridges linking Cu(II) into an one-dimensional chain architecture (Fig. 2b), and the separation of Cu…Cu is 10.80 Å. Owing to the weak Cu…O interactions, the1D chains and free H_2pdc ligands are extended into a two-dimensional layer architecture (Fig. 2c). In this layer, we can found that multipoint N-H…O hydrogen bonds further consolidate this 2D layer. Finally, such two-dimensional layers are stacked with the parallel manner *through* the weak forces of Van der Waals, providing a stacked three-dimensional supramolecular skeleton (Fig. 2d).

Powder X-ray diffraction (PXRD) patterns and thermogravimetric analyses (TGA)

The compounds phase purities purity was demonstrated via the analysis of PXRD, displayed in Fig. S1. Significantly, the pattern of experiment was in accordance with that of simulation created by the data of single crystal diffraction, clearly reflecting the excellent purities of massive samples.

Moreover, the compounds' thermal behaviors under nitrogen atmosphere were also characterized *via* the TGA experiments, and the TGA results are displayed in Fig. 3. In the TGA curve of **1**, the loss of the coordinated molecules of water appeared between 96 and 118 ℃ temperature (with the calculated and observed values of 5.70% and 5.72%), and subsequently, no remarkable weightlessness was found when the temperature less than 287 ℃, and then, the framework collapse appeared in the range of 287–416 ℃

that is on account of the organic ligand decomposition. In the compound **2**'s TGA curve, there is no evident weightlessness appeared when the temperature less than 290 ℃, and subsequently, rapid weightlessness occurred in the range of 290–433℃, revealing the framework collapse resulted from the organic ligand decomposition.

Photoluminescent property of 1

The luminescent spectra and free ligand of H_2pdc and the complex **1** were checked at environmental temperature. As displayed in the Fig. 4a, it can be found that the free ligand of H_2pdc reveals an emission band with the maximum peak at 436 nm (with λ_{ex} of 340 nm) that is owing to the orbital charge transitions of π^* to n or π [25], and compound **1** shows a much strong emission band, and at 447 nm, there exist the maximum peak (λ_{ex} = 340 nm). Owing to the d^{10} electronic configuration of Zn(II) ion, the **1**'s luminescence should principally derive from the π^* to n or π orbital charge transitions of pdc^{2-} ligand [26]. Compared to that of the H_2pdc ligand, a red-shift of 11 nm probably resulted from the H_2pdc ligand deprotonation and the pdc^{2-} ligand coordination to the central metal ions. By calculation, it can be found that the CIE chromaticity coordinate of **1** is (0.1689,0.1176) at the 1931 CIE chromaticity diagram (Fig. 4b), indicating that compound **1** may be served as an excellent blue fluorescent material.

Photocatalytic property of 2

The photocatalytic performance of 2 was evaluated by the degradation of methyl violet (MV) under UV light irradiation. As shown in Fig. 5a, it is clear that the absorption peak at about 580 nm of MV solution decreased gradually owing to the photodegradation of MV with the increase of irradiation time. After the irradiation time of 80 min, it can be calculated that 70.2% MV were successfully photodegraded by the photocatalyst of 2 (Fig. 5b). In addition, the control investigation without complex **2** was also implemented under the identical conditions, and the MV degradation reaction was relatively slow, and after 80 min, the leaving undegraded MV accounted for 84.9%. Such results indicated that compound 2 shows good activity for the MV photocatalytic degradation under the irradiation of ultraviolet light. Compared to the reported coordination polymers, the photocatalytic activity of 2 is little lower [27]. After photocatalytic reaction, compound 2 keeps the structural integrity that was proven via the patterns of PXRD (Fig. S1b).

Compound significantly reduce the expression levels of the NMDA receptor on neurons

Aspartic acid is an endogenous excitatory amino acid, which has a remarkable influence in the central nervous system of mammal, and the excessive accumulation of excitatory amino acids in the brain could lead to the PD development. Thus, in this present research, after the compound treatment, the expression levels of NMDA receptor on neurons were measured. As the outcomes illustrated in the Fig. 5, there was an evidently enhanced NMDA receptor expression level in contrast to control group. Nevertheless, after

treated with the **1**, expression levels of the NMDA receptor on neurons were decreased significantly, but the **2** exhibited nearly no effect on the NMDA receptor expression.

Compound obviously inhibited the levels of neurons apoptosis

In former investigation, we have suggested that the compound **1** could remarkably down-regulate the expression levels of NMDA receptor on neurons. However, the influence of the compound on the neurons' apoptosis was still need to be explored. The outcomes in the Fig. 6 revealed that in model group, the neurons apoptosis levels were much higher than control group. The **1** evidently decreased the apoptosis levels of neurons, which is much stronger than compound **2**.

Conclusions

On the whole, we have produced two fresh coordination polymers of $[Zn(pdc)(im)(H_2O)]_n$ (**1**) and $[Cu(pdc)(im)_2]_n \cdot n(H_2pdc)$ (**2**) (H_2pdc = terephthalic acid, im = imidazole). Both **1** and **2** have 1D chain structures. For **1**, the 1D chains are firstly linked via the N-H…O H-bonds into a 2D layer, which is interpenetrated by another adjacent identical one to form a bi-layer motif, and such bilayers are ultimately extended into a three-dimensional supramolecular skeleton *via* the connection of Ow-H…O H-bonds. For **2**, the 1D chains are firstly connected through the N-H…O H-bonds and weak Cu···O bonds into a 2D layer, and these two-dimensional layer are ultimately stacked into a three-dimensional supramolecular skeleton in a parallel mode. The intense blue luminescence of **1** and good photocatalytic activity of **2** indicate that they can be served as promising hybrid materials. Through the real time reverse transcription-polymerase assay, it can be found that the compound **1** possesses stronger inhibitory effect on decreasing the NMDA receptor expression levels against the neurons than **2**. Moreover, the **1** could evidently decrease the neurons apoptosis levels, which is better than the activity of compound **2**. In conclusion, compound **1** has good protein activity and is expected to be a candidate drug for the treatment of PD.

Declarations

Funding

Not applicable.

Conflicts of interest

The author(s) declare(s) that there is no conflict of interest regarding the publication of this paper.

Ethics approval

BALB/c mice (4-5 weeks, 20-22g) were used for PD animal model construction. Ethics Committee approval was obtained from the Institutional Ethics Committee of Model Animal Reach Center of Wuhan

University to the commencement of the study.

Consent to participate

This experiment does not involve clinical cases and informed consent.

Consent for publication

The authors agreed for the article publication.

Data availability

Selected bond lengths (Å) and angles (°) for compounds **1-2** (Table S1); The detailed hydrogen bond parameters for **1**-**2** (Table S2); The PXRD patterns (a) for compound **1** and (b) for compound **2** (Fig. S1), the information could be found in the supporting information file.

Code availability

Not applicable.

Authors' contributions

Ning Wang and Fang-Jie Huang synthesized and characterized the compounds; Mang-Suo Zhao and Bing-Xin Shi performed the activity assay experiments; Yan Wei and Li-Yan Qiao designed the study and prepared the manuscript.

References

1. Beitz JM. Parkinson's disease: a review. Front Biosci (Schol Ed). 2014; 6: 65-74.
2. Opara J, Małecki A, Małecka E, Socha T. Motor assessment in Parkinson`s disease. Ann Agric Environ Med. 2017; 24: 411-415.
3. Samii A, Nutt JG, Ransom BR. Parkinson's disease. Lancet. 2004; 363: 1783-1793.
4. M. Du, C. P. Li, C. S. Liu, S. M. Fang, Design and construction of coordination polymers with mixed-ligand synthetic strategy. Coord. Chem. Rev., 2013, 257, 1282-1305.
5. S. Kumar, R. P. Sharma, P. Venugopalan, V. S. Gondil, S. Chhibber, V. Ferretti, Synthesis and characterization of new silver(I) naphthalenedisulfonate complexes with heterocyclic N-donor ligands: Packing analyses and antibacterial studies. Polyhedron, 2019, 159, 275-283.
6. J. J. Huang, X. Zhang, Q. S. Huo, J. H. Yu, J. Q. Xu, 3,5-Bis((4'-carboxylbenzyl)oxy)benzoilate-based coordination polymers: their synthesis, structural characterization, and sensing properties. Inorg. Chem. Front., 2016, 3, 406-416.
7. T. Shi, Y. G. Chen, Syntheses, structures, and properties of two coordination complexes of a flexible ligand with channel structure. Z. Anorg. Allg. Chem., 2017, 643, 642-646.

8. Y. Qiao, X. Chang, J. Y. Zheng, M. Yi, Z. Chang, M. H. Yu, X. H. Bu, Self-interpenetrated water-stable microporous metal-organic framework toward storage and purification of light hydrocarbons. Inorg. Chem., 2021, 60, 2749-2755.
9. J. X. Li, Z. B. Qin, Y. H. Li, G. H. Cui, Visible-light-driven photocatalyst for the degradation of methylene blue over a 3D cobalt(II)-4,4'-oxybis(benzoate) framework. Inorg. Chem. Commun., 2018, 90, 112-114.
10. N. Bai, R. Gao, H. Wang, Y. Wu, L. Hou, Y. Wang, Five transition metal coordination polymers driven by a semirigid trifunctional nicotinic acid ligand: selective adsorption and magnetic properties. CrystEngComm, 2018, 20, 5726-5734.
11. Y. H. Tang, X. Wu, F. Wang, J. Zhang, Synthesis of zeolite-like metal-organic frameworks via a dual-ligand strategy. CrystEngComm, 2017, 19, 2549-2552.
12. L. Ma, Y. Y. Liu, F. Su, Self-assembly of Zn/Cd-coordination polymers based on 3,3',4, 4'-biphenyltetracarboxylic acid and N-donor ligands and luminescence sensing of Fe^{3+} ions. J. Solid State Chem., 2019, 269, 65-71.
13. F. Y. Yi, S. Dang, W. T. Yang, Z. M. Sun, Construction of porous Mn(II)-based metal–organic frameworks by flexible hexacarboxylic acid and rigid coligands. CrystEngComm, 2013, 15, 8320-8329.
14. Y. P. He, Y. X. Tan, J. Zhang, Tuning a layer to a pillared-layer metal–organic framework for adsorption and separation of light hydrocarbons. Chem. Commun., 2013, 49, 11323-11325.
15. Y. F. Liang, X. F. Wang, G. X. Zhang, Z. B. Han, A 2D Zn(II) coordination polymer constructed by right-handed and left-handed Zn–Hbci–Zn helical chains and μ_2-H_2O bridges (H_3bci=bis(2-carboxyethyl)isocyanurate)Inorg. Chem. Commun., 2011, 14, 1107-1110.
16. H. Yang, H. X. Zhang, D. C. Hou, T. H. Li, J. Zhang, Assembly between various molecular-building-blocks for network diversity of zinc–1,3,5-benzenetricarboxylate frameworks. CrystEngComm, 2012, 14, 8684-8688.
17. F. K. Wang, S. Y. Yang, R. B. Huang, L. S. Zheng, S. R. Batten, Control of the topologies and packing modes of three 2D coordination polymers through variation of the solvent ratio of a binary solvent mixture. CrystEngComm, 2008, 10, 1211-1215.
18. D. C. Hou, G. Y. Jiang, H. R. Fu, Z. Zhao, J. Zhang, A microporous nickel–organic framework with an unusual 10-connected bct net and high capacity for CO2, H2 and hydrocarbons. CrystEngComm, 2013, 15, 9499-9503.
19. T. Wang, L. Qin, C. L. Zhang, H. G. Zheng, Syntheses, characterization, and magnetic properties of novel divalent Co/Ni coordination polymers based on a V-shaped pyridine ligand and dicarboxylate acids. RSC Adv., 2015, 5, 64514-64519.
20. X. Zhang, Y. Y. Huang, J. K. Cheng, Y. G. Yao, J. Zhang, F. Wang, Alkaline earth metal ion doped Zn(II)-terephthalates. CrystEngComm, 2012, 14, 4843-4849.
21. Y. Song, B. Wang, Y. Liu, L. J. Guo, J. J. Cao, W. H. Li, T. Liu, S. Qiao, L. D. Guo, Heterometallic trinuclear cluster-based microporous metal-organic framework with high adsorption selectivity of

CO_2 over N_2. Inorg. Chem. Commun., 2020, 121, 108202.

22. Q. Liu, J. Y. Tan, J. Y. Zhang, N. Zhang, Z. J. Liu, Heterometallic metal-organic frameworks: two-step syntheses, structures and catalytic for imine synthesis. Micropor. Mesopor. Mat., 2021, 310, 110626.
23. G. M. Sheldrick, Crystal structure refinement with SHELXL. Acta Crystallogr., Sect. C: Struct. Chem., 2015, 71, 3-8.
24. X. Zhang, M. L. Sun, Y. Y. Huang, Y. G. Yao, Synthesis, structure, photoluminescence and theoretical calculation on a novel Zn(II) coordination polymer with (4,8)-connected topology. Inorg. Chem. Commun., 2013, 155-157.
25. D. Guo, C. M. Liang, K. Chiu, W. K. Wang, Bifunctional Sr(II)-terephthalate compound: gas adsorption and luminescence sensing properties. Z. Anorg. Allg. Chem., 2021, 647, 1-6.
26. Y. Zhang, K. Chen, Mixed solvothermal synthesis of a New heterometallic coordination polymer containing two distinct inorganic Cd–O–Ca chains. J. Inorg. Organomet. Poly. Mater., 2013, 23, 1049-1053.
27. Y. Zhang, W. Hu, C. Rao, D. Zhou, Y. Hu, J. Jin, M. Muddassir, Fast photocatalytic organic dye by two metal-organic frameworks with 3D two-fold interpenetrated feature. J. Mol. Struct., 2021, 1227, 129538.

Figures

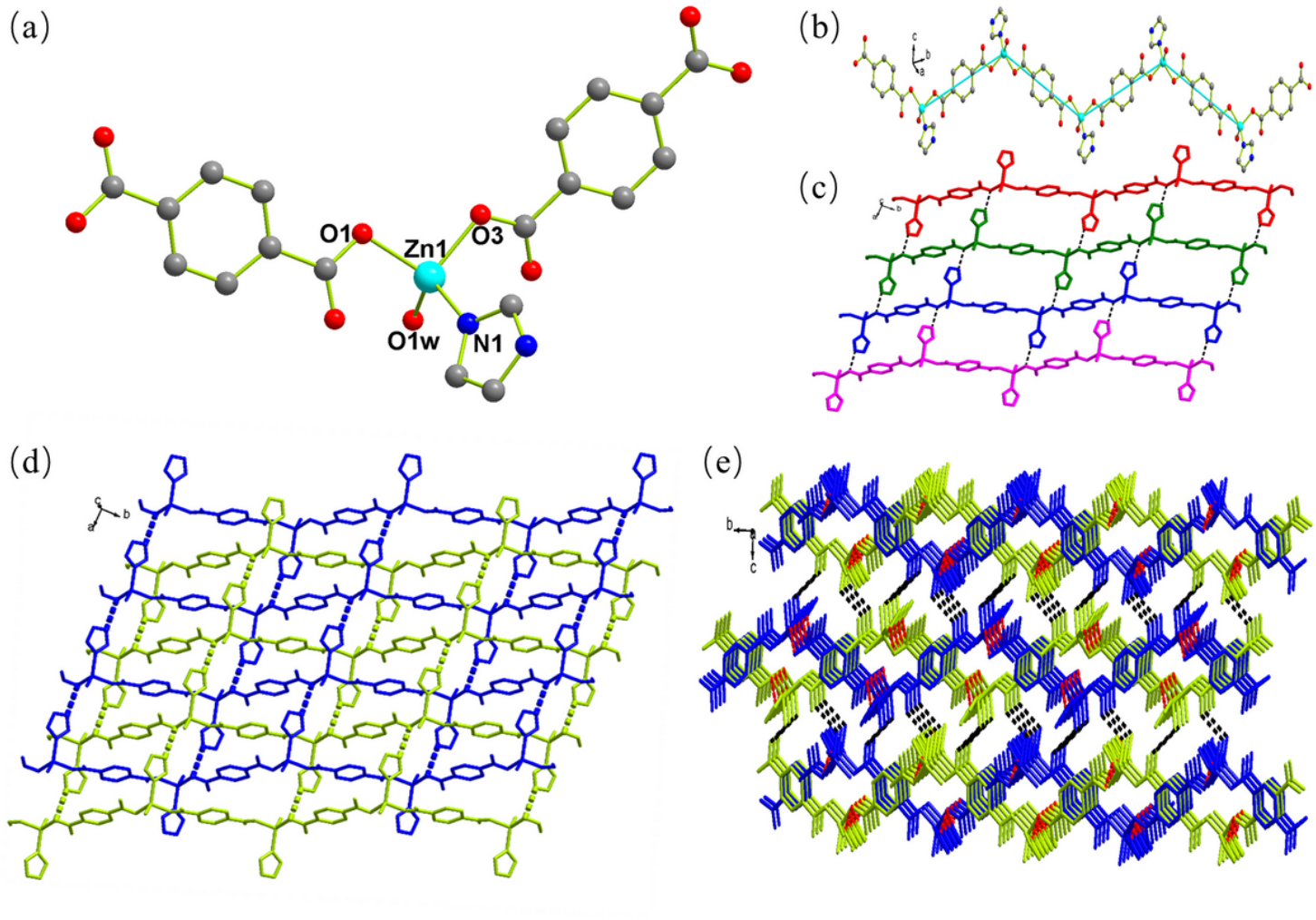

Figure 1

(a) The coordination surroundings view of Zn(II) ions in compound 1. (b) The one-dimensional infinite zigzag chain architecture of complex 1. (c) The N□H…O H-bonded two-dimensional layer. (d) The interpenetrated bi-layer. (e) The 1's three-dimensional supramolecular skeleton through the connection of Ow-H…O H-bonds.

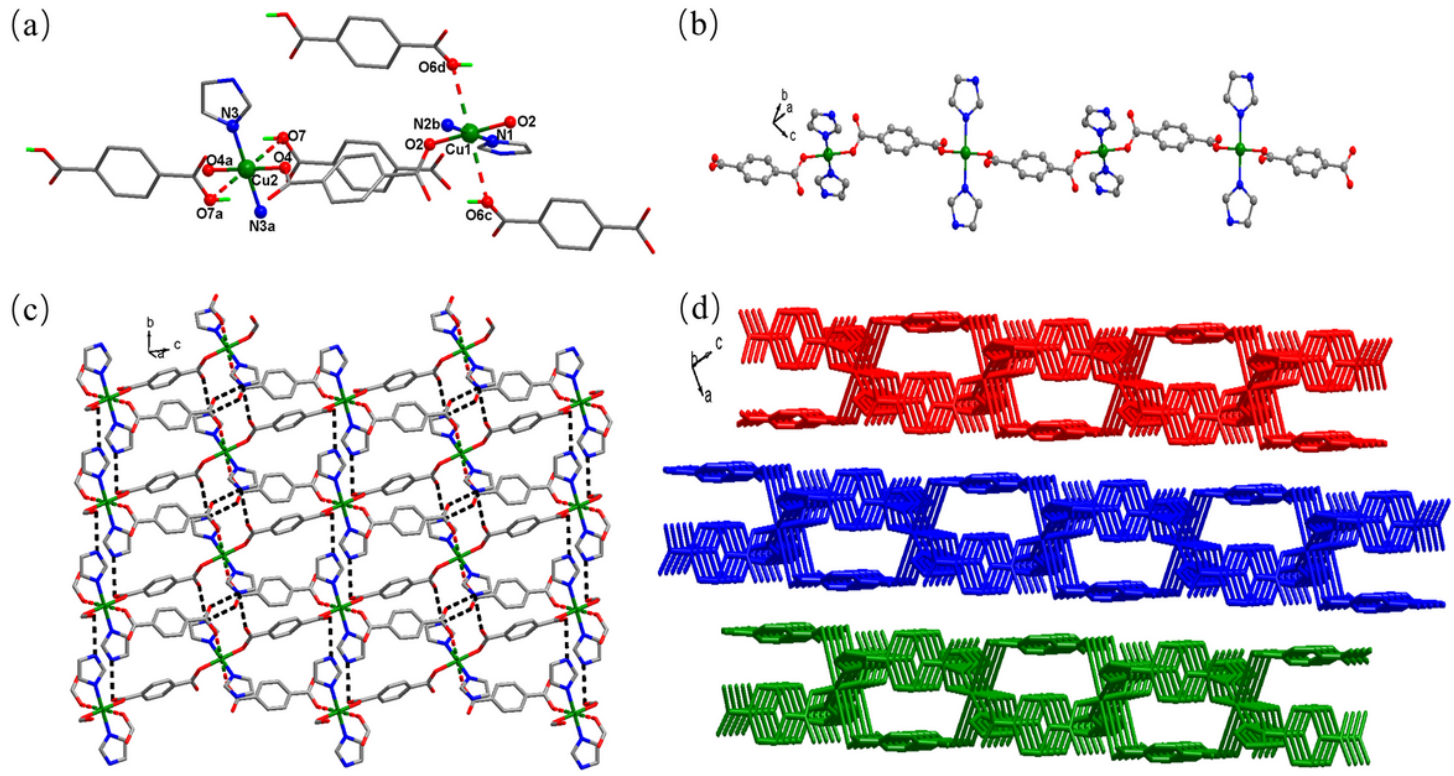

Figure 2

(a) The coordination surroundings of Cu(II) ions in compound 2. (b) The 2's one-dimensional infinite chain architecture. (c) The two-dimensional layer architecture by the connection of N□H…O H-bonds and weak Cu…O interactions. (d) The stacked 3D supramolecular framework for 2.

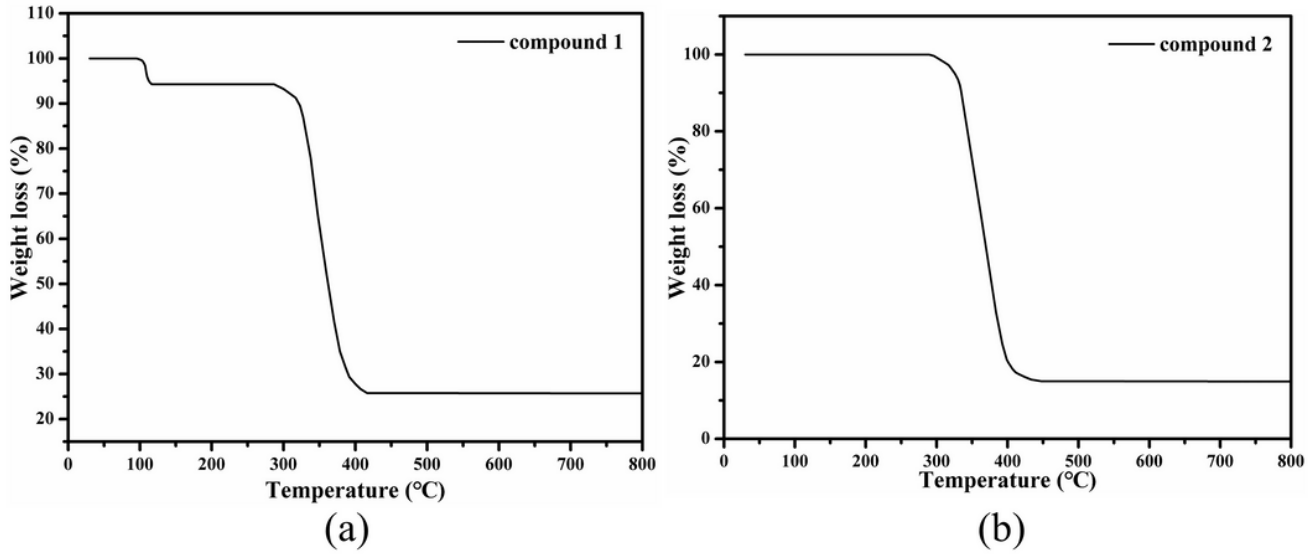

Figure 3

The curves of TGA (a) for complex 1 and (b) for complex 2.

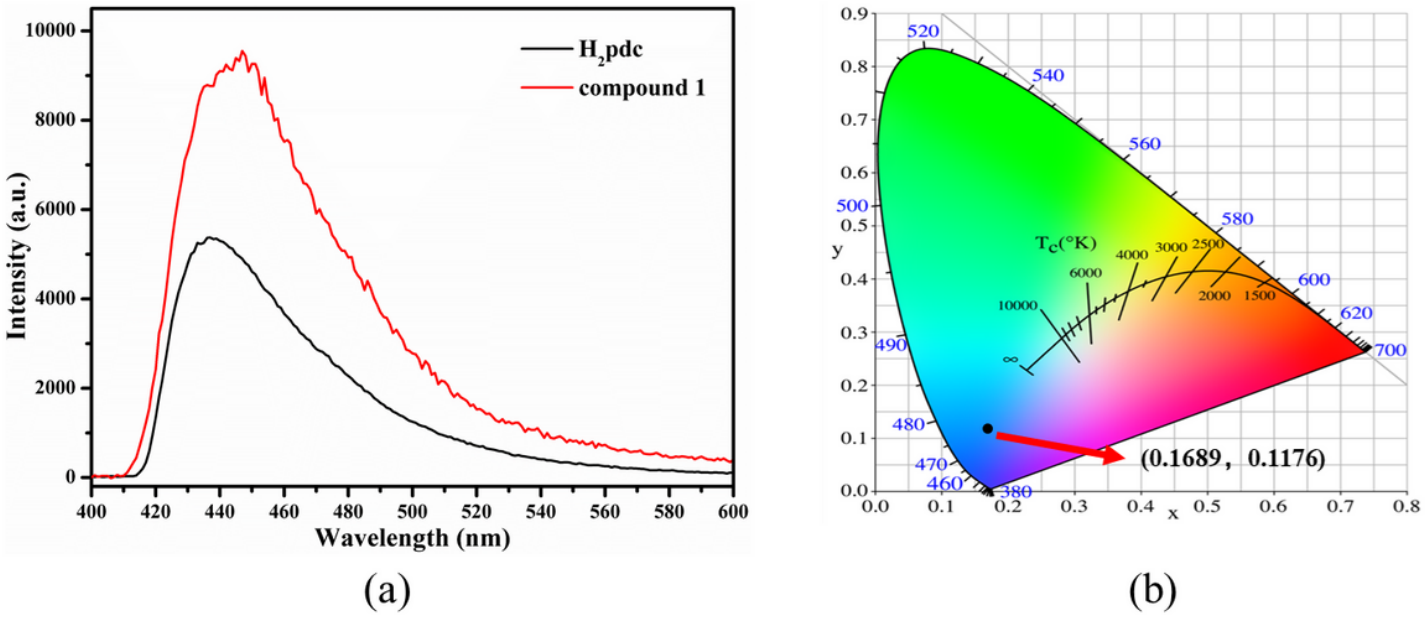

Figure 4

(a) The luminescent emission spectra of the ligand of H2pdc and complex 1 at environmental temperature. (b) The 1's diagram of CIE chromaticity.

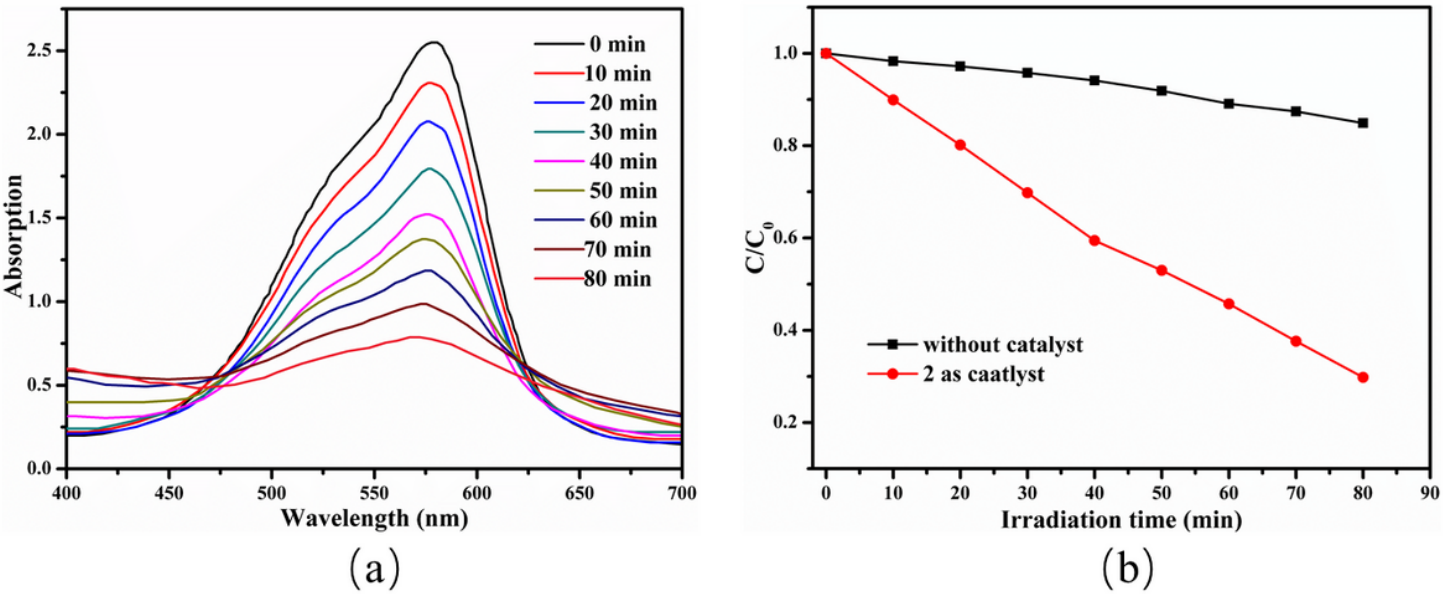

Figure 5

(a) Ultraviolet–visible absorption spectra for degradations of MV in the presence of 2 as photocatalyst. (b) The degradation rate of MV under UV light with or without 2 as photocatalyst.

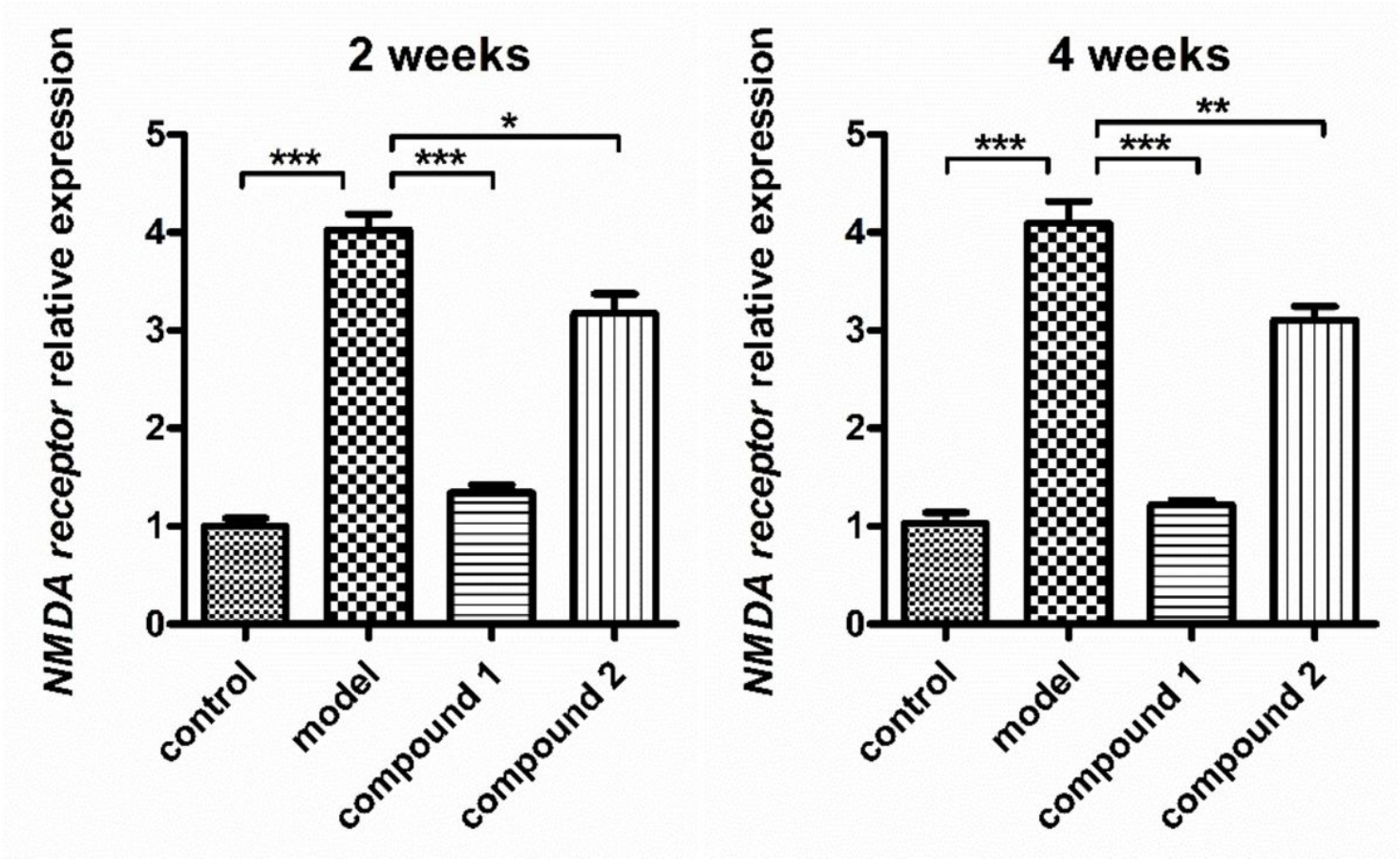

Figure 6

Significantly decrease NMDA receptor expression levels on the neurons after treating with compound. The PD animal model was created in our experiment, then the treatment of the two compounds was carried out with 5 mg per kg concentration. The expression levels of NMDA receptor on neurons was assessed through the real time RT-PCR.

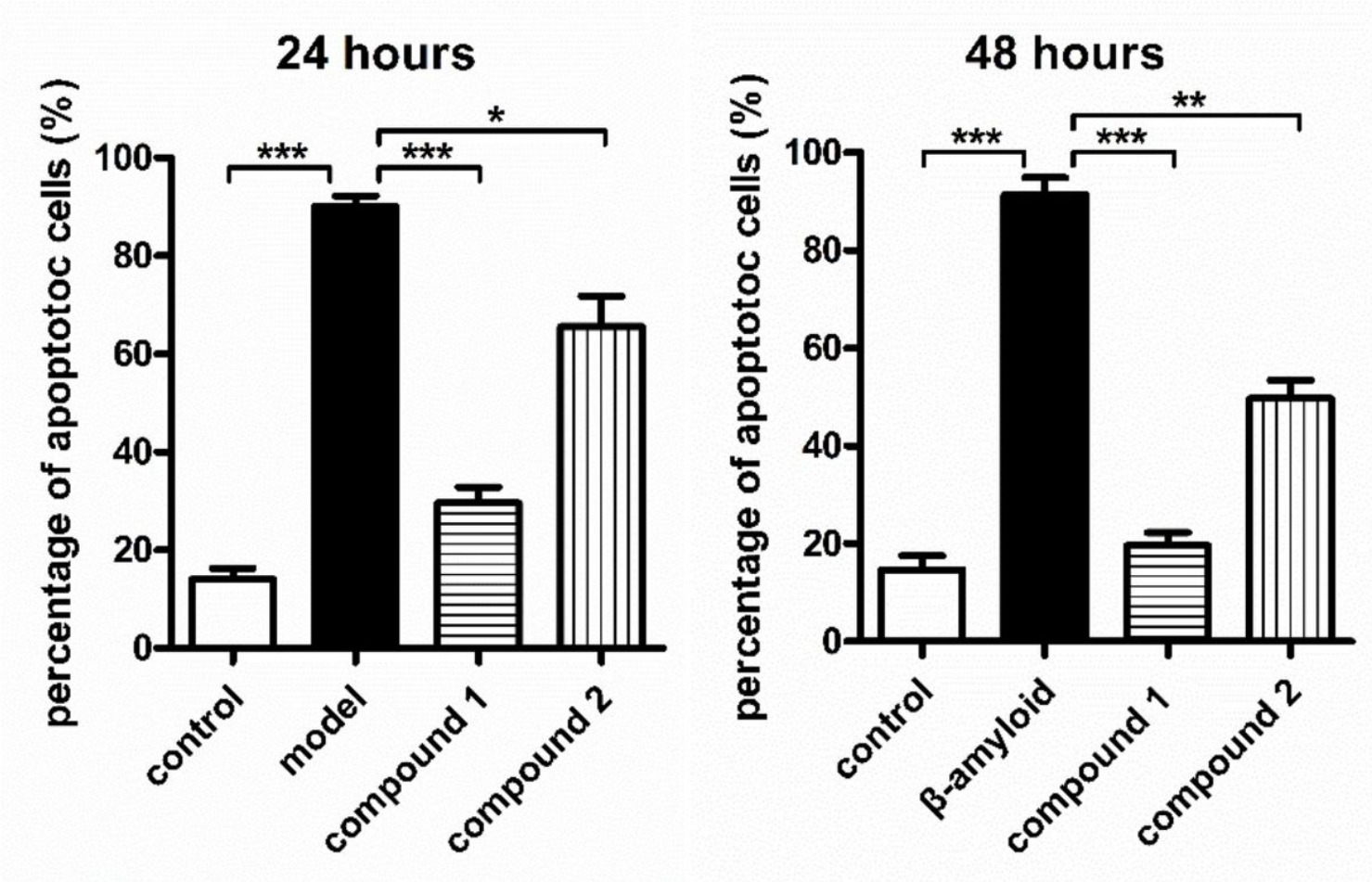

Figure 7

Obviously inhibited levels of neurons apoptosis after compound's treatment. The PD animal model was created in our experiment, then the treatment of the two compounds was carried out with 5 mg per kg concentration. The assessment of apoptotic neurons levels was finished with apoptosis assay of Annexin V-FITC/PI.

Supplementary Files

This is a list of supplementary files associated with this preprint. Click to download.

- SupplementaryMaterial.doc